Mon. Not. R. Astron. Soc. **394,** 214–220 (2009) doi:10.1111/j.1365-2966.2008.13504.x

Optical observations of GRB 050401 afterglow : a case for double-jet model

Atish Kamble,[1,2]★ Kuntal Misra,[3,4] D. Bhattacharya[1,4] and Ram Sagar[3]

[1]*Raman Research Institute, Bangalore – 560 080, India*
[2]*Astronomical Institute "Anton Pannekoek", Kruislaan 403, 1098 SJ Amsterdam, The Netherlands*
[3]*Aryabhatta Research Institute of Observational Sciences, Manora Peak, Nainital – 263 129, India*
[4]*Inter University Centre for Astronomy and Astrophysics, Post Bag 4, Ganeshkhind, Pune – 411 007, India*

Accepted 2008 May 27. Received 2008 May 9; in original form 2007 January 25

ABSTRACT

The afterglow of GRB 050401 presents several novel and interesting features. (i) An initially faster decay in optical band than in X-rays. (ii) A break in the X-ray light curve after ∼0.06 d with an unusual slope after the break. (iii)The X-ray afterglow does not show any spectral evolution across the break while the *R*-band light curve does not show any break. We have modelled the observed multiband evolution of the afterglow of GRB 050401 as originating in a two-component jet, and interpreting the break in X-ray light curve as due to lateral expansion of a narrow collimated outflow which dominates the X-ray emission. The optical emission is attributed to a wider jet component. Our model reproduces all the observed features of multiband afterglow of GRB 050401. We present optical observations of GRB 050401 using the 104-cm Sampurnanand Telescope at the Aryabhatta Research Institute of Observational Sciences (ARIES), Nainital. Results of the analysis of multiband data are presented and compared with GRB 030329, the first reported case of double jet.

Key words: gamma-rays: bursts.

1 INTRODUCTION

The optical and X-ray light curves of Gamma Ray Burst (GRB) afterglows, in the simplest cases, show a power-law decay with an index $\alpha \sim 1.0$. Deceleration of the relativistic shock wave generated by the explosion, which results in GRB, can explain the power-law decay of the GRB afterglows. The most common deviation from the power-law decay behaviour of the afterglow light curves is an achromatic break seen in the light curve. This break has been seen in a significant number of GRB afterglows and has been successfully explained as being due to the sideways expansion of the collimated ejecta from the explosion. In the post-*Swift* era, many more deviations from this simple behaviour of the afterglow-light curve have been detected. *Swift* with its capabilities of quick slewing towards the source has been able to observe GRB afterglows as early as a few tens of seconds after the burst. In this early part of the evolution, the GRB afterglows commonly exhibit a steep decay with $\alpha \sim 3$–5, with the usual definition $F_\nu(t) \propto t^{-\alpha}\ \nu^{-\beta}$, where $F_\nu(t)$ is the observed afterglow flux at frequency 'ν' and time t. The phase of the steep decay lasts for about a few hundred seconds after which a slower decay, with $\alpha \sim 0.5$, of the afterglow starts. About a few thousands of seconds after the burst, the afterglow starts decaying steeply again with $\alpha > 1.0$.

Many GRB afterglows observed by *Swift* show puzzling features in the light curves like (i) early steep decay (α ∼3-5) and (ii) Chromatic breaks (breaks seen in some wavebands but not others) with $\Delta\alpha$ ∼1.0 which are difficult to explain using the standard fireball model (Rees & Meszaros 1992; Meszaros & Rees 1993). It has been shown by O'Brien et al. (2006), Willingale et al. (2006) that the puzzling features of the X-ray afterglow-light curves can be fitted using one or two components with exactly the same empirical functional form, viz. an exponential fall followed by a power-law decay of flux with time, although it has not yet resulted into any physical understanding of the behaviour of the X-ray afterglow. While there is no clear understanding of the early steep decays of GRB afterglows, a few plausible explanations have been put forward: see for example Zhang et al. (2006) and Pe'er, Mészáros & Rees (2006). The flat decay of X-ray afterglow-light curves which follows the steep decay have been, in some cases, explained as being due to energy injection from the central engine, probably a magnetar (Zhang & Mészáros 2001, 2002). From the study of chromatic breaks seen in six well-sampled afterglow-light curves Panaitescu et al. (2006) concludes that if both, the optical and the X-ray afterglows, were to arise from the same outflow then the chromaticity of light-curve breaks can rule out energy injection or the structure of the jet as the possible reasons of it.

One such GRB afterglow with puzzling features in optical and X-ray light curves is GRB 050401. GRB 050401 triggered *Swift*-BAT (Burst Alert Telescope)at 14:20:15 UT on 2005 April 01 (Barbier et al. 2005). The X-ray afterglow was detected by

★E-mail: akamble@science.uva.nl

Swift-XRT (Angelini et al. 2005) about 130 s after the trigger and the optical afterglow candidate was confirmed by ground-based observations by Price & McNaught (2005). The burst duration T_{90} is estimated to be ∼33 s (Sakamoto et al. 2005). Using the measured spectral redshift of the afterglow ($z = 2.9$) (Fynbo et al. 2005) and the fluence (Golenetskii et al. 2005; Sakamoto et al. 2005; De Pasquale et al. 2006), the isotropic equivalent energy released during the explosion turns out to be 1.4×10^{54} for a flat universe with $\Omega_m = 0.3$, $\Omega_\Lambda = 0.7$ and $H_0 = 70\,\mathrm{km\,s^{-1}\,Mpc^{-1}}$. multiband afterglow of GRB 050401 also presents some puzzling features which can be summarized as follows.

(i) A break in the X-ray light curve after ∼0.06 d with an unusual slope after the break (Watson et al. 2005; De Pasquale et al. 2006).

(ii) The X-ray afterglow does not show any spectral evolution across the break while the *R*-band light curve does not show any break (Watson et al. 2005; De Pasquale et al. 2006).

(iii) A large extinction inferred from X-ray afterglow which is not consistent with the observed optical afterglow (Watson et al. 2005).

The optical observations are presented in Section 2. We have done some preliminary analysis of the light curves, which is discussed in Section 3. We have tried to explain the multiband behaviour of the GRB afterglow using a double-jet model, which is described in Section 4 along with the previous attempts by others using a different model. In the Discussion section (Section 5), molecular clouds as a plausible explanation for the large extinction are presented (Section 5.1). The only other GRB afterglow which has been explained using a similar double-jet model is the GRB 030329 (Berger et al. 2003; Resmi et al. 2005). We compare the physical features of GRB 030329 and GRB 050401 in Section 5.2. Our conclusions are summarized in Section 6.

2 OPTICAL OBSERVATIONS AND DATA REDUCTION

Optical observations of the afterglow of GRB 050401 were carried out in the broad and Johnson V and Cousins RI filters using the 104-cm Sampurnanand Telescope of the Aryabhatta Research Institute of Observational Sciences (ARIES), Nainital on 2005 April 01. The gain and read out noise of the CCD camera are 10 e^-/ADU and 5.3 e^-, respectively. The data have been binned in 2×2 pixel^2 to improve the signal-to-noise ratio. The bias subtracted, flat fielded and cosmic ray removed images were processed and analysed using MIDAS,[1] IRAF[2] and DAOPHOT (Stetson 1987) softwares.

The Landolt (1992) standard region SA 107 and the OA field in *B*, *V*, *R* and *I* filters were observed on 2005 May 16 for photometric calibration during good photometric sky conditions. The values of atmospheric extinction on the night of 2005 May 16/17 determined from the observations of SA 107 bright stars are 0.26, 0.18, 0.13 and 0.10 mag in *B*, *V*, *R* and *I* filters, respectively. The seven-standard stars in the SA 107 region cover a range of $0.339 < (V - R) < 0.923$ in colour and $12.116 < V < 14.884$ in brightness.

Using these transformation coefficients, we determine BVRI magnitudes of 18-secondary stars in GRB 050401 field and their average values are listed in Table 1. The (*X*, *Y*) CCD pixel coordinates were converted to α_{2000}, δ_{2000} values using the astrometric positions given by Henden (2005). The 18-secondary stars in the field of GRB 050401 were observed 2–4 times in *B*, *V*, *R* and *I* filters. These stars have internal photometric accuracy better than 0.01 mag. The zero-point differences on comparison between our photometry and that of Henden (2005) are 0.15±0.08, 0.09±0.04, 0.10±0.05 and 0.54±0.29 mag in *B*, *V*, *R* and *I* filters, respectively. These differences are based on the comparison of the six-secondary stars in the GRB 050401 field.

The afterglow magnitudes were differentially calibrated with respect to the secondary stars listed in Table 1. The magnitudes derived in this way are given in Table 2.

[1] MIDAS is distributed by the European Southern Observatories. Visit : www.eso.org/esomidas/

[2] IRAF is distributed by the National Optical Astronomy Observatories, USA. Visit : http://iraf.noao.edu/

Table 1. The identification number (ID), (α, δ) for epoch 2000, standard *V*, ($B - V$), ($V - R$) and ($V - I$) photometric magnitudes of the stars in the GRB 050401 region are given.

ID	α_{2000} (h m s)	δ_{2000} (° m s)	*V* (mag)	$B - V$ (mag)	$V - R$ (mag)	$V - I$ (mag)
1	16 31 20.01	02 06 52.9	17.28	0.64	0.35	0.84
2	16 31 23.84	02 07 44.3	16.87	0.77	0.52	0.98
3	16 31 29.22	02 08 13.8	17.66	1.14	0.75	1.40
4	16 31 37.63	02 08 07.3	16.78	0.69	0.46	0.87
5	16 31 40.12	02 10 30.1	16.35	0.58	0.38	0.73
6	16 31 36.96	02 11 36.5	18.23	0.97	0.62	1.12
7	16 31 32.61	02 12 38.7	17.68	0.41	0.34	0.67
8	16 31 24.79	02 13 35.4	19.56	1.37	1.08	2.29
9	16 31 18.94	02 13 12.1	19.21	1.26	0.83	1.60
10	16 31 18.56	02 12 40.8	15.30	0.85	0.51	0.93
11	16 31 22.46	02 11 13.7	15.61	0.69	0.46	0.87
12	16 31 21.38	02 10 43.0	15.51	0.88	0.53	0.99
13	16 31 19.42	02 09 56.3	14.60	0.55	0.36	0.69
14	16 31 15.08	02 09 19.1	14.34	0.61	0.38	0.74
15	16 31 23.42	02 09 13.7	16.39	0.66	0.44	0.83
16	16 31 17.26	02 07 58.9	16.17	0.63	0.41	0.81
17	16 31 15.93	02 07 36.6	18.91	1.16	0.89	1.75
18	16 31 14.79	02 07 14.6	17.54	0.74	0.47	0.93

Table 2. The optical observations of the afterglow of GRB 050401 using the 104-cm Sampurnanand Telescope at ARIES, Nainital. ΔT in column two refers to the time after the burst in days. The effective-exposure time after combining all the images turns out to be 900 s for individual passbands reported here.

Date (UT) 2005 April	ΔT (d)	Magnitude (mag)	Passband
01.8824	0.2850	22.33 ± 0.347	*V*
01.8324	0.2850	21.43 ± 0.231	*R*
01.8698	0.2724	20.51 ± 0.207	*I*

3 LIGHT CURVES OF GRB 050401 AFTERGLOW

Along with our own observations, we have used observations reported elsewhere to study the light curves of GRB 050401. The X-ray light curve of GRB 050401 was obtained from Watson et al. (2005). The optical observations by Watson et al. (2005) have been calibrated by observing a Landolt field. We do not have detailed information about this calibration. Hence, to take into account any uncertainties associated with it, we have added an error of 0.2 mag in the optical observations reported by Watson et al. (2005).

Another set of optical observations is taken from Rykoff et al. (2005), the calibration of which is roughly equivalent to the R_c-band system. We add a small error of 0.1 mag to all these observations by Robotic Optical Transient Search Experiment (ROTSE-III) to take into account the calibration uncertainties.

Very Large Array reported a 4σ detection of a source at the position of GRB 050401 (Soderberg 2005) with intensity of 122 μJy at 8.46 GHz about 5.7 d after the burst. Other attempts, including by the Giant Metrewave Radio Telescope (GMRT) in India at 610 MHz (Chandra & Ray 2005) and by the Australia Telescope Compact Array (ATCA) in Australia at 8.5 GHz and 4.8 GHz (Saripalli et al. 2005), to observe the radio afterglow of GRB 050401 could produce only upper limits.

To construct the optical-light curve, we have corrected the observed magnitudes for the standard Galactic extinction law given by Mathis (1990). The Galactic extinction in the direction of GRB 050401 is estimated to be $E(B-V) = 0.065$ mag from the smoothed reddening map provided by Schlegel, Finkbeiner & Davis (1998). The effective wavelength and normalization given by Bessell, Castelli & Plez (1998) were used to convert the magnitudes to fluxes in μJy.

Most of the GRB afterglow-light curves are well characterized by a broken power law of the form

$$F = F_0\{(t/t_b)^{\alpha_1 s} + (t/t_b)^{\alpha_2 s}\}^{-1/s}, \quad (1)$$

where α_1 and α_2 are the afterglow flux decay indices before and after the break time (t_b), respectively. F_0 is the flux normalization and 's' is a smoothening parameter which controls the sharpness of the break. Most known GRB afterglows have $\alpha_1 \sim 1$ and $\alpha_2 > \alpha_1$ that is the decay becomes steeper after the break.

The X-ray and optical (R band) afterglow of GRB 050401 are very well sampled over a wide period of observation. The available R-band observations cover a duration from 36 s to 13 d after the burst, while the X-ray observations range from ∼130 s to 12 d after the burst. The X-ray afterglow-light curve shows a prominent break near 0.06 d while the optical afterglow does not show any such break in the light curve. We analyse this behaviour in detail below.

(i) The X-ray light curve shows a clear break near 0.06 d. The change of slope across the break is significant. Fitting equation (1) to the data yield the decay slopes
$\alpha_{X1} = 0.58 \pm 0.02$ for $\Delta t < 0.06$ d;
$\alpha_{X2} = 1.37 \pm 0.03$ for $\Delta t > 0.06$ d.
The change of slope across the break, $\Delta\alpha_X \sim 0.8$, is therefore quite substantial.

(ii) The optical afterglow shows a monotonic decay with decay index $\alpha_R = 0.82 \pm 0.02$ over the entire period of observation (up to 13 d). There is no evidence of a break simultaneous with that in the X-ray light curve.

(iii) According to the standard-fireball model of GRB afterglows, the X-ray light curve is expected to decay at least as fast as the optical-light curve which is indeed true for the majority of GRB afterglows observed so far. In the case of GRB 050401, we find that the X-ray afterglow shows a decay slower than optical-light curve till ∼0.06 d after which it decays at a much faster rate as described above.

Thus, the relatively slow initial decay of optical and X-ray light curves, presence of a break in X-ray light curve and absence of such a break in optical, and initially slower decay of the light curve in X-rays than in optical bands make the afterglow of GRB 050401 an unusual and interesting one.

4 MODELLING OF GRB 050401 AFTERGLOW

The change in slope across the break in the X-ray light curve $\Delta\alpha_X \sim 0.8$ is too large to be explained by the passage of a spectral break. In the standard-fireball model of GRB afterglows, the passage of the cooling break ν_c through the observing band leads to a steepening of light curve by an amount of $\Delta\alpha_X = 0.25$, much smaller than that is observed for GRB 050401 afterglow, along with the change of spectral slope by $\Delta\beta_X = 0.5$. The X-ray spectrum of GRB 050401 does not exhibit any change in the spectral slope across the break. We thus rule out the possibility of ν_c passing through the X-ray band at the time of break.

De Pasquale et al. (2006) explain the initial flatter decay and the break in the X-ray light curve based on a model by Zhang & Mészáros (2001, 2002). According to this model, the central engine of GRB remains active for several thousand seconds after the burst, continuously injecting energy into the fireball. If the central engine is injecting energy above a certain critical rate then it can slow down deceleration of the shock wave which results in a shallow decay of the light curve. The break in the light curve occurs when the central engine stops injecting sufficient amount of energy into the fireball. After this epoch, the afterglow can be described using standard fireball model giving $\alpha = (3/2)\beta$. Being a dynamical effect, the end of energy injection episode would result in an achromatic break in the afterglow-light curves. Although this model seems to explain the X-ray light curve reasonably well, but absence of a similar break in optical afterglow-light curve is sufficient to rule this model out for GRB 050401.

Watson et al. (2005) point out another puzzle : the soft X-ray absorption implies an equivalent optical extinction of magnitude $A_V = 9.1^{+1.4}_{-1.5}$ mag in the host galaxy, assuming solar abundance.

However, if the optical and the X-ray emission are part of the same synchrotron spectrum, then A_V is constrained to be ∼1.45 for no spectral break between optical and X-rays and $A_V < 0.67$ if a cooling break exists in between [a Small Magellanic Cloud (SMC) extinction law is assumed]. These values are highly discordant with that predicted from X-ray absorption. Watson et al. (2005) suggest that this may indicate a on-universal dust-to-metals ratio which they estimate to be more than a factor of 10 less than that in the SMC.

Watson et al. (2005) remark that the only alternative to this highly anomalous dust to metal ratio is separate emission regions for the optical and X-rays. We explore this possibility assuming that two distinct jet components give rise to the observed emission in these two (X-ray and optical) wavelength bands. The jet contributing to the X-ray emission is narrow, exhibiting an early break while that contributing to the optical emission is wider. The optical contribution from the narrow jet is strongly diminished due to the presence of high extinction $A_V \sim 9$ along the line of sight, while the wider jet suffers from a smaller degree of average extinction.

4.1 Spectral parameters of the afterglow of GRB 050401

The radiation spectrum of a GRB afterglows exhibits a power-law spectrum characterized by three break frequencies – the self-absorption frequency ν_a, the peak frequency ν_m corresponding to the lower cut-off (γ_m) in the electron-energy distribution ($n(\gamma_e) \propto \gamma_e^{-p}$, $\gamma_e > \gamma_m$, where γ_e is the Lorentz factor of the radiating electrons) and the synchrotron cooling frequency ν_c. The flux F_m at ν_m provides the normalization of the spectrum (Sari, Piran & Narayan 1998).

The photon index (Γ) of the X-ray afterglow is related to its spectral index (β), $\Gamma - 1 = \beta$, which in turn is related to the

electron-energy distribution index p in any given spectral regime ($\beta = p/2$ if $\nu_c < \nu_X$ and $\beta = (p-1)/2$ if $\nu_X < \nu_c$). The corresponding temporal decay index α_X would be $(3p-2)/4$ and $3(p-1)/4$, respectively, before the jet break and p in both spectral regimes after the jet break, according to the standard fireball model for an afterglow expanding in a homogeneous interstellar medium. In the present case, the observed values of α_X are consistent with $p = 1.42$ and a jet break around 0.06 d after the burst. However, we note that the observed value of the spectral-photon index $\Gamma \sim 1.85 \pm 0.03$ (Watson et al. 2005) implies a steeper $p \sim 1.7 \pm 0.06$. It should also be noted that from analysis of the same data set of X-ray observations, De Pasquale et al. (2006) infer $\beta = 0.75 \pm 0.15$ for PC mode data after the break at 0.06 d. This β is consistent with $p = 1.42$ that we inferred above.

The optical (R band) afterglow, on the other hand, exhibits a temporal slope $\alpha_R = 0.82$ which, in the commonly encountered spectral regime of $\nu_m < \nu_R < \nu_c$, implies $p = 2.1$. This is different from that inferred for the X-ray afterglow, and indeed regardless of the choice of spectral regimes, it is not possible to produce both α_X and α_R from the same underlying power-law energy distribution of injected electrons. One possibility, therefore, is that the optical and the X-ray afterglows originate in physically distinct outflows. We consider two physically distinct components of the outflow, such as the coaxial jets, one having a dominant contribution in the optical and the other in the X-rays, giving rise to the observed afterglow of GRB 050401.

Table 3. Best-fitting spectral parameters for the afterglow of GRB 050401 assuming two-component jet model described in Section 4. Light curves generated using these parameters and their subsequent evolution according to the standard fireball model are plotted in Fig. 1. All the parameters are calculated at 0.01 d after the burst. GRB 050401 was at redshift $z = 2.9$.

	Narrow jet	Wider jet
ν_m(Hz)	$2.0^{+1.2}_{-0.81} \times 10^{13}$	$1.1^{+1.53}_{-0.83} \times 10^{13}$
ν_c(Hz)	$4.1 \pm 0.9 \times 10^{14}$	$5.25^{+30.0}_{-5.0} \times 10^{15}$
$F_{peak}(\mu Jy)$	2140^{+210}_{-230}	1750^{+1050}_{-950}
t_{jet}(day)	0.06 ± 0.03	–
p	1.42 ± 0.02	$2.1^{+0.2}_{-0.11}$
$E(B-V)_{Host}$	4.1	$0.23^{+0.22}_{-0.13}$
$\chi^2_{d.o.f.}$ (d.o.f.)	1.2 (85)	

We then fit the full, multiband-light curves of GRB050401 with those predicted by a double-jet model using linear least square method. Results of this fit are displayed in Fig. 1, and the best-fitting values of various spectral parameters are listed in Table 3. We note that the contribution of the narrow jet to the optical afterglow is

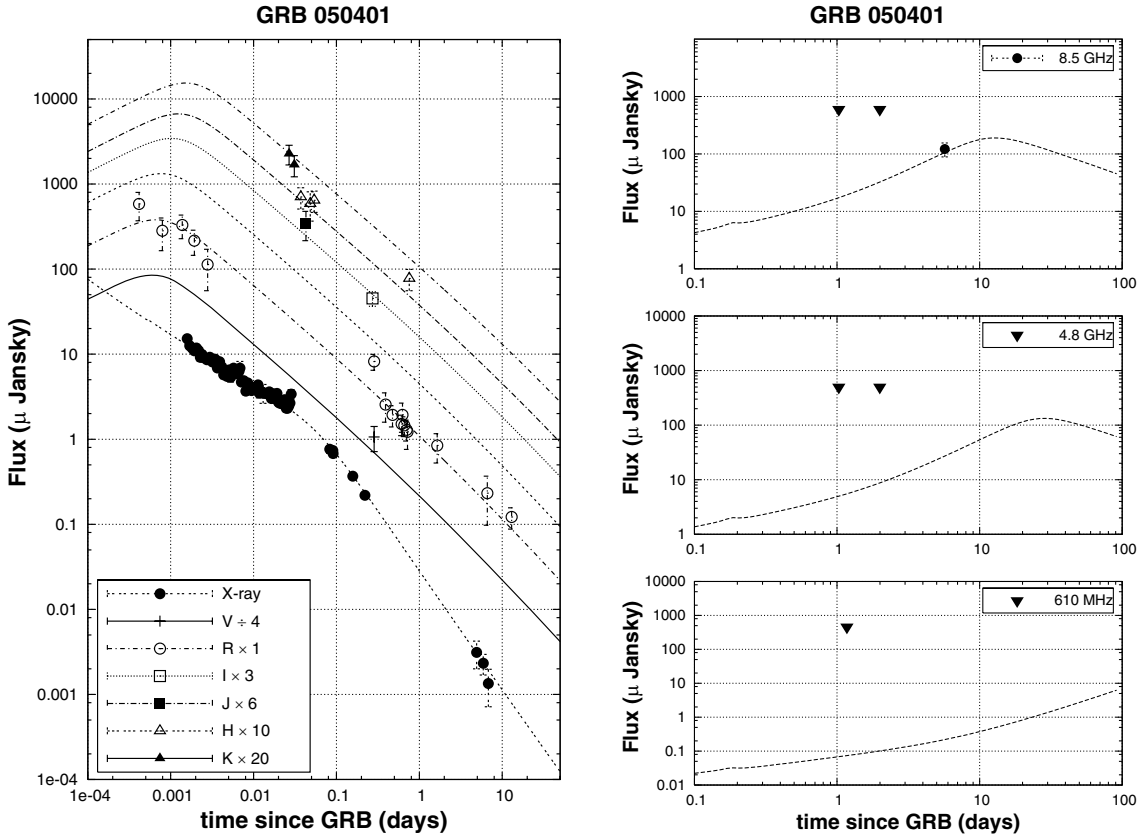

Figure 1. The observed optical and X-ray light curves (left-hand panel) and radio-light curves (right-hand panel)of GRB 050401 afterglow compared with the double-jet model fit (solid lines). The steepening of X-ray afterglow-light curves at 0.06 d after the burst is explained as a jet break due to the lateral expansion of a narrow jet which has a dominant contribution in X-rays. The surrounding wider jet contributes dominantly in optical. Since, no break in the optical-light curves is observed till 13 d after the burst, the wider jet is expected to be $> 29^\circ$. Our best-fitting model gives the value of electron-energy distribution index within the narrow jet to be $p = 1.42$ and that within the wider jet to be $p = 2.1$. The peak in the optical-light curves corresponds to the passage of ν_m through the observing band. The radio upper limits are indicated by filled triangles in the right-hand panels. The sole radio detection at 8.5 GHz is indicated by a filled circle. The solid lines in the right-hand panels are the light curves expected from the best-fitting spectral parameters. The corresponding frequencies are listed in a rectangle at the top right corner of each box.

Table 4. The physical parameters for the afterglow of GRB 050401 assuming a two-component jet model described in Section 4. The quantity $E_{52}^{\rm iso}$ is the isotropic equivalent energy in units of 10^{52} ergs. The corresponding collimation corrected energy is $E_{52}^{\rm corr}$ in units of 10^{52} ergs.

	Narrow jet	Wider jet
n	$14.7^{+10.5}_{-5.34}$	$20^{+2583}_{-19.3}$
$\epsilon_{\rm e}$	$(2.3 \pm 0.6) \times 10^{-2}$	$(4^{+6}_{-2}) \times 10^{-2}$
ϵ_B	$5^{+4}_{-2} \times 10^{-4}$	$1^{+9}_{-0.9} \times 10^{-3}$
$E_{52}^{\rm iso}$	53.23 ± 16.2	$1.34^{+1.36}_{-0.82}$
θ_j	$1.15^\circ \pm 0.15^\circ$	$> 29^\circ$
$E_{52}^{\rm corr}$	$(1.1 \pm 0.2) \times 10^{50}$	$>6.5 \times 10^{50}$

strongly suppressed due to large extinction. The X-ray afterglow, on the other hand, is modified as a sum of the emission from both the jets, with the narrow jet being the dominant contributor. For the narrow jet, we find a best-fitting value of $p = 1.42$. For the wider jet, which dominates the optical afterglow of GRB 050401, we estimate $p = 2.1$. The extinction that the radiation from the narrow jet encounters is fixed at $A_V = 9.1$ as derived from the soft X-ray absorption (Watson et al. 2005), while that for the wide jet is treated as a fit parameter.

4.2 Physical Parameters for GRB 050401

Four spectral parameters ($\nu_{\rm a}$, $\nu_{\rm m}$, $\nu_{\rm c}$ and $F_{\rm peak}$) are related to four physical parameters viz. n (number density of the circumburst medium), E (total energy content of the fireball), energy fraction in relativistic electrons $\epsilon_{\rm e}$ and that in magnetic field ϵ_B. The typical value of self-absorption frequency $\nu_{\rm a}$ lies in radio-mm waves and hence is best estimated only if the afterglow is well observed in these bands. Unfortunately, the afterglow of GRB 050401 was detected only once at the radio band (Soderberg 2005) which is not sufficient to determine $\nu_{\rm a}$ accurately. We therefore converted the remaining three spectral parameters into the four physical parameters using $\epsilon_{\rm e} = \sqrt{\epsilon_B}$ as an additional constraint. The choice of this relation is motivated by Medvedev (2006). When $p < 2.0$, as it is in the present case of narrow jet, a high energy cut-off for the electron-energy distribution is required and the expressions for spectral parameters, as given in Wijers & Galama (1999), have to be modified accordingly. The modifications have been provided by Bhattacharya (2001) which we have used for estimating the physical parameters in the present case. We estimate the density of the circumburst medium to be $n \approx 10$ and $\epsilon_{\rm e} = \sqrt{\epsilon_B} = 0.03$ for both the jets. The physical parameters estimated for both the jets are listed in Table 4. Using the $E^{\rm iso}$ and n, and the jet-break time in X-rays $t_j = 0.06$ d, we find the opening angle of the narrow jet to be quite small, 1.15°. Since there is no jet break seen in the optical-light curve till $\sim$13 d, a lower limit on the opening angle of the wider jet is derived to be 29°. The collimation-corrected kinetic energies are $E^{\rm K}_{\rm wide} > 6.5 \times 10^{50}$ ergs and $E^{\rm K}_{\rm narrow} = 1.1 \times 10^{50}$ ergs.

5 DISCUSSION

5.1 A plausible explanation for the large extinction inferred from X-ray absorption

It is now well established from the observations of GRB hosts that long GRBs preferentially occur in massive star-forming regions, for example Woosley & Bloom (2006). The massive star-forming regions host large-molecular clouds. Typical column densities of cold-molecular clouds are $>10^{22}\,{\rm cm}^{-2}$, densities $100 - 10^4\,{\rm cm}^{-3}$ and sizes $\sim$20 pc. Giant-molecular clouds are even denser (10^4–$10^7\,{\rm cm}^{-3}$) and larger ($\sim$100 pc) (Shore 2002). It is possible that one such cloud in the host galaxy of GRB 050401 happens to fall along our line of sight which can explain the large-extinction inferred from the X-ray spectrum. We consider the possibility of radiation from the double jet of GRB 050401 being obscured by a molecular cloud so aligned that it covers the narrow jet of GRB 050401 completely while the wide jet is partially covered. By changing the fractional coverage of wide jet by the cloud, we measured change in the value of reduced χ^2 of the fit. In effect, this amounts to adjusting the intrinsic luminosity of the wide jet upwards with increasing covering factor to match the observed optical flux. This results in the relative contribution of the wide jet to the X-ray afterglow to increase, affecting the fit quality. Keeping all other parameters fixed at their best-fitting values obtained for zero coverage, we find that a covering fraction of 60 per cent can be accommodated within a range of $\Delta\chi^2/{\rm d.o.f.} = 1$. Beyond this the reduced χ^2 rises sharply and reaches $\Delta\chi^2/{\rm d.o.f.} > 15$ for a covering factor of $\sim$90 per cent. For the observed column density of $1.7 \times 10^{22}\,{\rm cm}^{-2}$ (De Pasquale et al. 2006) and assuming typical densities (100–1000 ${\rm cm}^{-3}$) of the molecular clouds, the size of the molecular cloud could be estimated to be around 5–55 ${\rm s}^{-1}$. It is therefore probable that one such molecular cloud partially obscures our view of GRB 050401. This situation is illustrated in Fig. 2.

At this point, we would like to point out two possible caveats in the double-jet model proposed here.

The separation of the optical and X-ray emitting regions, as proposed in the present model, is motivated by the large discrepancy of about 8 mag between the amount of optical extinction inferred from soft X-ray absorption and that from observed optical-inferared spectrum of the GRB050401 afterglow. It should, however, be kept in mind that the Predehl & Schmitt (1995) relation used to predict A_V from X-ray absorbing column $N_{\rm H}$ is an empirical one, and cannot be considered fully reliable in all circumstances. For example, a metallicity higher than solar by a factor of 10, or a dust-to-gas ratio lower by a similar factor, can reconcile the X-ray absorption with observed optical extinction. Such explanations in this case cannot be ruled out, and have been already discussed by Watson et al. (2005).

The second caveat is that the model presented here requires a rather special geometrical alignment – the two jets of the GRB should shine through the outer edge of a molecular cloud, much larger in size than the transverse extent of the jet-working surface, in such a manner as to provide large extinction to the inner jet but much less to at least half the outer component. This requires that the outer edge of the cloud be dense, and have a strong-density gradient to differentially affect the two-jet components. An elongated, cigar-shaped cloud with its axis nearly parallel to the line of sight, would also help such a scenario. We also note that the size of the cloud required, as estimated by us using an average density, is prone to large uncertainties if its shape is unusual or if large-density gradients are present.

5.2 GRB 050401 and GRB 030329 : a comparison

The only other GRB whose afterglow has been explained as being due to double jet is the GRB 030329 (Berger et al. 2003; Resmi et al. 2005). Optical and X-ray light curves of GRB 030329 afterglow showed a near simultaneous break at 0.55 d whereas the

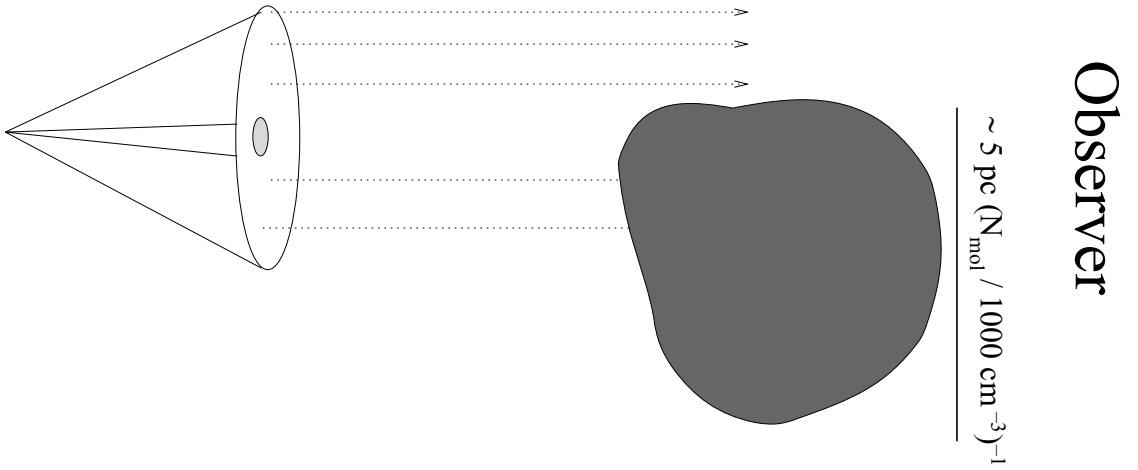

Figure 2. A side view of the double jet (not to scale). The observer is on the axis of the jets and at a distance of 24 Gpc (which can be considered as at infinity for geometric purposes in this figure). The arrows indicate the afterglow-light rays emanating from the jets. The intervening-molecular cloud, of size larger than 5–55 pc, responsible for the observed large extinction is sitting at a distance of about 100–1000 pc from the GRB. The estimated diameters of the jets around 0.05 d turn out to be about 2×10^{-3} and $>2 \times 10^{-2}$ pc, respectively, for the narrow and the wide jet. The large cloud covers a significant portion of the central narrow jet and partially covers the wide jet when seen from the observer's point of view. As a result, the optical radiation from the narrow jet is completely extincted. Most of the optical radiation from the wide jet does not suffer from this extinction.

radio-light curves had a break at about 10 d after the burst. Berger et al. (2003) have explained the two breaks as being due to lateral expansion of the two coaxial jets of different opening angles ($\sim$5° and $\sim$17°).

In the case of GRB 050401, afterglow-light curves do not show the presence of two different breaks. Instead, absence of a break at optical frequencies till late times ($\sim$13 d after the burst) leads us to infer the presence of a wider jet with opening angle larger than 29° while a steep break ($\Delta\alpha \sim 0.8$) at 0.06 d after the burst in X-ray light curve can be explained as a jet break due to lateral expansion of a narrow jet of opening angle 1.15°.

The wider jet of GRB 030329 was estimated to be marginally more energetic than the narrower jet (Berger et al. 2003; Resmi et al. 2005). Similarly, in the case of GRB 050401, we find that the wider jet is marginally more energetic than the narrower jet.

5.3 GRB 050401 and the Ghirlanda relation

It has been found that the collimation corrected energies (E_γ) of the GRBs are correlated with the peak energy of the GRB spectrum as measured in the frame of reference of the source ($E^{\rm src}_{\rm peak}$). This correlation is also called as the Ghirlanda relation (Ghirlanda, Ghisellini & Lazzati 2004). Unfortunately, the $E^{\rm src}_{\rm peak}$ for GRB 050401 is not available as it falls outside the energy range of BAT. However, Sato et al. (2007) have used the Konus–Wind spectral data to find $E^{\rm obs}_{\rm peak}$. From their analysis, Sato et al. (2007) find that in order to satisfy the Ghirlanda relation the afterglow-light curve of GRB 050401 should exhibit a jet break $\sim 10^4$ s after the burst. This lower limit of the allowed range for jet break time is close to the break seen at 0.06 d in the X-ray light curve of GRB 050401, which we interpret as a jet break corresponding to the narrow jet in our model.

Sato et al. (2007) quantify the Ghirlanda relation as $E^{\rm src}_{\rm peak} = A\,E^{0.706}_{\gamma,52}$, where $E_{\gamma,52}$ is the collimation-corrected energy released in γ rays during the burst, in units of 10^{52} ergs. Using a sample of a large number of GRBs Sato et al. (2007) constrain the value of the proportionality constant A : $1950 < A < 4380$. Using the estimated value of $E^{\rm iso}_\gamma \sim 10^{54}$ ergs and the 1.15° as the opening angle of the narrow jet in our double-jet model, the E_γ turns out to be 2×10^{50} ergs. Using $E^{\rm src}_{\rm peak} = 447^{+75}_{-64}$ keV for GRB 050401 as reported by Sato et al. (2007) along with $E_\gamma = 2 \times 10^{50}$ ergs we estimate $A = 7076^{+2597}_{-1897}$. This value of A is within 2σ of $A = 4380$, the higher limit on A obtained considering the sample of GRBs satisfying the Ghirlanda relation. Having discussed this, we would also like to point out that the Ghirlanda relation has sometimes been criticized as being due to selection effects rather than being an intrinsic correlation (Butler, Kocevski & Bloom 2008).

6 SUMMARY

We have reported *VRI*-band observations of GRB 050401 afterglow on 2005 April 1. Also, we have modelled the afterglow of GRB 050401 as due to two physically distinct collimated outflows, using our own *VRI*-band photometry along with the observations available in the literature, and compared with GRB 030329. Our main conclusions about GRB 050401 are as follows.

(i) We showed that the light curves of GRB 050401 afterglow can not be explained under the assumption of continuous energy injection. The flatter decay, which appealed for the continuous energy-injection model, can instead be explained by low values of electron-energy distribution index p.

(ii) The afterglow of GRB 050401 can be well fit by the double-jet model with the interpretation that the break in the X-ray light curve at $\sim$0.06 d after the burst is due to a narrow collimated jet expanding sideways. The obscured optical emission is attributed to a wider which did not undergo significant sideways expansion until at least $\sim$13 d after the burst.

(iii) Kinematically, we find that the wider jet is slightly more energetic, than the narrow jet. This result is similar to what was found in the double jet of GRB 030329.

(iv) Our interpretation of the break in the X-ray light curve at 0.06 d after the burst as a jet break is consistent with the Ghirlanda relation.

ACKNOWLEDGMENTS

We are thankful to the anonymous referee for his/her detailed comments, which have improved the paper significantly. This research has made use of data obtained through the High Energy Astrophysics Science Archive Research Centre Online Service, provided by the NASA/Goddard Space Flight Centre. We acknowledge the use of public data from the *Swift* data archive. Two of the authors AK and KM acknowledge the support received from Dept. of Science and Technology, Govt. of India.

REFERENCES

Angelini L. et al., 2005, GCN, 3161
Barbier L. et al., 2005, GCN, 3162
Berger E. et al., 2003, Nat, 426, 154
Bessell M. S., Castelli F., Plez B., 1998, A&A, 333, 231
Bhattacharya D., 2001, Bull. Astron. Soc. India, 29, 107
Butler N. R., Kocevski D., Bloom J., 2008, preprint (arXiv:0802.3396)
Chandra P., Ray A., 2005, GCN, 3178
De Pasquale M., Beardmore A. P., Barthelmy S. D. et al., 2006, MNRAS, 365, 1031
Fynbo J. P. U. et al., 2005, GCN, 3176
Ghirlanda G., Ghisellini G., Lazzati D., 2004, ApJ, 616, 331
Golenetskii S., Aptekar R., Mazets E., Pal'shin V., Frederiks D., Cline T., 2005, GCN, 3179
Henden A., 2005, GCN, 3454
Landolt A. U., 1992, AJ, 104, 340
Mathis J. S., 1990, ARA&A, 28, 37
Medvedev M. V., 2006, ApJ, 651, L9
Meszaros P., Rees M. J., 1993, ApJ, 418, L59
O'Brien P. T. et al., 2006, ApJ, 647, 1213
Panaitescu A., Mészáros P., Burrows D., Nousek J., Gehrels N., O'Brien P., 2006, MNRAS, 369, 2059
Pe'er A., Mészáros P., Rees M. J., 2006, ApJ, 652, 482
Predehl P., Schmitt J. H. M. M., 1995, A&A, 293, 889
Price P. A., McNaught R., 2005, GCN, 3164
Rees M. J., Meszaros P., 1992, MNRAS, 258, 41P
Resmi L. et al., 2005, A&A, 440, 477
Rykoff E. S. et al., 2005, ApJ, 631, L121
Sakamoto T. et al., 2005, GCN, 3173
Sari R., Piran T., Narayan R., 1998, ApJ, 497, L17
Saripalli L., Wu K., Ghosh K. K., Swartz D. A., Tennant A. F., 2005, GCN, 3177
Sato G. et al., 2007, ApJ, 657, 359
Schlegel D. J., Finkbeiner D. P., Davis M., 1998, ApJ, 500, 525
Shore S. N., 2002, The Tapestry of Modern Astrophysics, John Wiley & Sons, New York
Soderberg A. M., 2005, GCN, 3187
Stetson P. B., 1987, PASP, 99, 191
Watson D. et al., 2006, ApJ, 652, 1011
Wijers R. A. M. J., Galama T. J., 1999, ApJ, 523, 177
Willingale R. et al., 2007, ApJ, 662, 1093
Woosley S. E., Bloom J. S., 2006, ARA&A, 44, 507
Zhang B., Mészáros P., 2001, ApJ, 552, L35
Zhang B., Mészáros P., 2002, ApJ, 566, 712
Zhang B., Fan Y. Z., Dyks J., Kobayashi S., Meszaros P., Burrows D., Nousek J., 2006, ApJ, 642, 354

This paper has been typeset from a TEX/LATEX file prepared by the author.